DENTAL MATERIALS 35 (2019) 862–870

Available online at www.sciencedirect.com

ScienceDirect

journal homepage: www.intl.elsevierhealth.com/journals/dema

Influence of bioactive glass-coating of zirconia implant surfaces on human osteoblast behavior in vitro

Nadja Rohr[a,b,*], *J. Barbara Nebe*[b], *Fredy Schmidli*[a], *Petra Müller*[b], *Michael Weber*[c], *Horst Fischer*[c], *Jens Fischer*[a]

[a] *Division of Dental Materials and Engineering, Department of Reconstructive Dentistry, University Center for Dental Medicine, University of Basel, Basel, Switzerland*

[b] *Department of Cell Biology, University Medical Center Rostock, Rostock, Germany*

[c] *Department of Dental Materials and Biomaterials Research, RWTH Aachen University Hospital, Aachen, Germany*

ARTICLE INFO

Article history:
Received 25 October 2018
Received in revised form
14 February 2019
Accepted 27 February 2019

Keywords:
Zirconia implant
Bioglass coating
Human osteoblasts
Microstructure

ABSTRACT

Objective. The recently developed bioactive glass PC-XG3, which is suitable to coat zirconia implant surfaces with high adhesion strength may reduce the time of osseointegration and the marginal bone loss following implantation. The glass composition has been previously evaluated for cytotoxicity on fibroblast cells, and will now be used to evaluate the cell behavior of osteoblast cells.

Methods. Three different surface morphologies were created with PC-XG3 on zirconia discs. A clinically tested zirconia implant surface as well as polished and machined zirconia served as a reference. Cell viability after 24 h, cell spreading after 30 min and 24 h and the respective morphology of human osteoblasts using scanning electron microscopy were evaluated. Additionally, the corrosive process of PC-XG3 in cell culture medium up to 7 d was measured.

Results. Initial cell behavior of human osteoblasts was not accelerated by the PC-XG3 surface when compared to zirconia. Additionally, it was found that a decreased surface roughness promoted initial cell spreading. Storage in cell culture medium resulted in the accumulation of C and N on the bioglass surface while Mg, Si, K and Ca were decreased and crack formation was observed.

Significance. Since initial spreading quality to a biomaterial is a crucial factor that will determine the subsequent cell function, proliferation, differentiation, and viability it can be assumed that a coating of zirconia implants with this bioactive glass will unlikely reduce osseointegration time.

* *Corresponding author at*: Division of Dental Materials and Engineering, Department of Reconstructive Dentistry, University Center for Dental Medicine, University of Basel, Hebelstrasse 3, CH-4056, Basel, Switzerland.
E-mail address: nadja.rohr@unibas.ch (N. Rohr).

https://doi.org/10.1016/j.dental.2019.02.029

1. Introduction

Dental implants made of zirconia can be considered an esthetic and biocompatible alternative to the well-established titanium implants [1–5]. Zirconia is however susceptible to tensile stress and displays a high elastic modulus of 210 GPa [6]. To accelerate osseointegration, surface modifications of the endosseous part of the implant are created using different techniques. For titanium it has been shown that the implant surface should be moderately roughened with an Ra of 1 to 2 μm to increase bone implant contact and resistance to torque [7]. For zirconia implants a micro-structuring of the endosseous implant part has therefore also been postulated. Zirconia implants pre-treated with sandblasting, hydrofluoric acid etching [8] or laser, are currently available. However, three-year data on the clinical performance of commercially available zirconia implants only exists for the sandblasted, hydrofluoric acid etched ZLA surface (pure, Straumann, Basel, Switzerland) [5] and additionally heat treated cer.face 14 surface (ceramic implant, vitaclinical, VITA, D-Bad Säckingen) [4].

The production of a cer.face 14 zirconia implant surface is very time consuming, expensive and etching with 40 % hydrofluoric acid a potential health risk to the technical operator. The etching procedure is, however, required to create a micro-structured surface to increase the implants torque and achieve its osseointegration.

Balmer et al. revealed that a certain immediate loading of zirconia implants is possible without crestal bone loss [4]. It would be attractive to both, dentist and patient if the final restoration were placed directly after implant insertion using the technique to establish an appropriate emergence profile recommended by Lambert and Mainjot [9]. This would eliminate additional appointments with the patient and therefore significantly reduce time and costs. If the osseointegration process could be accelerated even faster to guarantee the successful placement of the final restoration with immediate loading directly after inserting the implant, the efficiency of zirconia implant placement could be significantly increased. Therefore, in order to improve the clinical concept, further research on how to improve the quality of osseointegration and reduce healing time by optimizing the surface morphology of zirconia implants is of high priority.

To address the mentioned requirements and potentially slow down the marginal bone loss following implantation coatings made of bioactive glasses can be applied onto the implant surfaces [10–12].

Bioactive glasses are able to create a direct chemical bond to bone over the formation of hydroxyl carbonated apatite on its surface [13,14]. The mechanism is initiated by the rapid dissolution of alkalis from the glass surface when in contact with aqueous solutions. A Ca-rich and P-rich layer at the inner alkali-depleted silica layer and consequently, a layer of hydroxyapatite or hydroxyl carbonated apatite is created on the glass surface [12]. The bioglass itself undergoes degradation over time when in contact with body fluids, being gradually replaced by new bone [13]. The corrosion kinetic depends on the glass network structure, type of ions present in the glass and dissolution medium [13]. Thus, 45–52 % of SiO_2 content in bioglasses are reported to feature fast bonding rates to tissue within 5–10 days [13,15].

Table 1 – Zirconia specimens were prepared or coated with bioglass PCX-G3 as given in the table to create differing micro-structured surfaces.

Code	Surface
Zp	Zirconia, sintered, hot isostatically pressed, polished
Zm	Zirconia, sintered, hot isostatically pressed
Z14	Zirconia, cer.face 14
G1	PCX-G3, sintered 830 °C 100 min
G2	PCX-G3, sintered 830 °C 100 min + sintered 760 °C 10 min
G3	PCX-G3, sintered 830 °C 100 min + sintered 750 °C 25 min

Bioglass 45S5 invented in the late 1960s by Hench LL, is still considered as the gold standard of bioactive materials [12,16]. However, due to its high crystallization tendency and the high coefficient of thermal expansion (CTE) of 15.1×10^{-6} K^{-1} [11], Bioglass 45S5 is not suitable for a thermal coating process on zirconia with a CTE of 10.8 to 12.5×10^{-6} K^{-1} [17,18]. Therefore, the glass composition of Bioglass 45S5 has recently been modified by a partial substitution of Na_2O and CaO by K_2O and MgO to display a similar thermal expansion as zirconia [19]. This absorbable glass called PC-XG3 also contains Ca^{2+} and PO_4^{3-} that potentially contribute to the mineralization process. Smooth and micro-structured glass coatings of PC-XG3 were applied on polished zirconia surfaces with promising results [19]. The glass coating revealed a strong adhesion to the zirconia substrates as well as a significant bioactive behavior in simulated body fluid (SBF) in in vitro experiments. The cell proliferation of L929 mouse fibroblasts on the PC-XG3 glass was similar to the one on bioglass 45S5 and both displayed a very low cytotoxicity of around 10% [19]. A complete dissolution of a layer of 50 μm of PC-XG3 when in contact to artificial saliva can be expected within 30 days. In a next step the osteoblast behavior on the bioactive glass PC-XG3 has to be analyzed to evaluate its potential for improving the osseointegration behavior.

The objective of the present study was therefore to evaluate osteoblast behavior on bioactive glass PC-XG3 and to further characterize its corrosion. Three differently micro-structured glass coatings were created and compared to polished and machined zirconia as well as the clinically tested cer.face 14 implant surface. Hypothesis were that (1) cell viability of human osteoblasts will be increased on PC-XG3 coated surfaces compared to zirconia surfaces and (2) cell spreading will be accelerated on PC-XG3 surfaces compared to zirconia surfaces.

2. Materials and methods

2.1. *Specimen production*

Six different surface morphology options for a zirconia implant surface were compared in the present study (Table 1). Sintered and hot isostatically pressed yttria-stabilized zirconia specimens with a diameter of 13 mm and a height of 2 mm were provided by the manufacturer (VITA Zahnfabrik, Bad Säckingen, Germany). These specimens were used with an as machined, sintered and hot isostatically (Zm) as well

as with an additionally polished surface (Zp). The surface of a zirconia implant ("cer.face 14"), with documented clinical success [4] was provided by the manufacturer of the implant (Z14). To create the Z14 structure, the zirconia substrates were sandblasted, etched with 40% hydrofluoric acid and heat treated as previously described [8]. Zirconia specimens were coated one (G1) or two times (G2, G3) with bioactive glass PC-GX3 [14]. This bioglass coating is composed of 45 wt% SiO_2, 22.5 wt% CaO, 17.0 wt% MgO, 9.5 wt% K_2O, and 6.0 wt% P_2O_5 and has its dilatometric softening point at 730.5 °C while crystallization starts at 910 °C [19]. The bioglass was synthesized out of 37.8 wt% SiO_2, 9.7 wt% $CaHPO_4$, 26.6 wt% $CaCO_3$, 14.3 wt% MgO and 11.7 wt% K_2CO_3 using the melt quench technique at 1400 °C for 2 h. Glass frits were dried at 70 °C for 18 h and then powdered using ZrO_2 balls over 24 h, sieved (<710 μm) powdered again over 20 d and sieved (<20 μm). Prior to the bioglass coating the zirconia surfaces were subjected to a cleaning firing at 800 °C for 10 min (Austromat 3001, Dekema, Freilassing, Germany). Specimens were then coated with bioactive glass using a custom-made device (built using fischertechnik, Waldachtal, Germany). Briefly, the glass powder of PC-GX3 was suspended with distilled water (1:1), 1 wt% binding agent (Optapix G1201, Zschimmer & Schwarz, Lahnstein, Germany) and 0.25 wt% wetting agent (KG 9033, Zschimmer & Schwarz) and then immediately sprayed on the specimens. Twenty zirconia specimens were therefore placed on a disc that passed the spray nozzle (model 97; Düsen-Schlick, Untersiemau, Germany) that was driven with a pressure of 0.5 bar in a distance of 35 mm with 22 rpm. To achieve a coating thickness of 20 μm of the specimens, the device was programmed to pass the drizzle 16 times while being automatically dried in-betweens for 5 s with a ventilator."

After drying for 15 min at room temperature (RT), all coated specimens of G1, G2, and G3 were sintered at 830 °C for 100 min (Austromat 3001). For G2 and G3 a second layer of bioglass was applied on the densely sintered first coating and fired at 760 °C for 10 min (G2) or 750 °C for 25 min (G3) respectively to create a microstructure. The amorphous bioglass coatings had a thickness of 20–40 μm after sintering. The thickness was checked with light microscopy (AXIO Imager M2m, Zeiss, Wetzlar) after coating as well as after sintering by breaking one specimen per batch in half using a universal testing machine (Z020, Zwick/Roell, Ulm Germany) with a cross-head speed of 50 mm/s. All specimens were finally cleaned in an ultrasonic bath with ethanol 70 % for 5 min, followed by distilled water for 5 min, sterilized at 200 °C for 2 h (T 5028, Heraeus, Hanau, Germany) and then stored in sterile 24-well-plates. Storage time after manufacturing of specimens until measurements was at least 2 weeks.

2.2. *Surface characterization*

The surface topography of the specimens was visualized using scanning electron microscopy (SEM) (ESEM XL30, Philips, Eindhoven, the Netherlands). Specimens were gold-sputtered with a layer of 20 nm and images captured at 1000× from 3 angles deviating by 10° to additionally visualize 3D topography (Alicona MeX, Alicona Imaging v 6.1). Based on the 3D SEM images, roughness parameters arithmetical mean height (Sa) and maximum height (Sz) was calculated (filter tc λc 20.0 μm; area 7000 μm).

To verify 3D data also 2D roughness parameters arithmetical mean height (Ra) and maximum height of profile (Rz) were measured with a profilometer (T1000/TKK50, Hommelwerke, Schwenningen, Germany). For each group 6 specimens were analyzed with 5 contact measurements over a distance of 4.8 mm (T1E, tip 5 μm 90°, 1.6 mN, Hommel-Etamic/Jenoptik, Jena, Germany). Surface wetting was measured using contact angle of water (WCA) with a drop-shape-analyzer (DSA100, Krüss, Hamburg, Germany). Five sessile drops of 0.5 μl were measured on 6 specimens per group. To evaluate the corrosion of the glass-coated surfaces, an energy-dispersive X-ray analysis (EDX) (Genesis, EDAX, Mahwah, NJ, USA/XL30 FEG ESEM, Philips Electron Optics, Eindhoven, The Netherlands) was conducted on G1–G3 at 20 kV after manufacturing and after storage in complete cell culture medium (see below, DMEM + 10%FCS) of 37 °C for 30 min, 24 h, 3 d and 7 d, respectively. Additionally, surfaces were observed for crack development using SEM. To evaluate the corrosion depth of the glass coating on the zirconia surfaces, specimens of G1–G3 were broken in half at a cross-head speed of 50 mm/min using a universal testing machine (Z020, Zwick/Roell, Ulm, Germany).

2.3. *Cell behavior*

2.3.1. *Cell cultivation*

Cell behavior of human osteoblast-like cells (MG-63) was tested on all surfaces. MG-63 cells (American Type Culture Collection ATCC, CRL1427) were cultivated in Dulbecco's modified eagle medium (DMEM; gibco, Thermo Fisher Scientific, Waltham, USA) with 10 % fetal calf serum (FCS, Biochrom FCS superior, Merck KGaA, Darmstadt, Germany) and 1% antibiotic (gentamicin, ratiopharm, Ulm, Germany). Specimen surfaces were seeded with 5×10^4 MG-63 cells (passages 8–23, 70–80 % confluent) and incubated in 24-well plates at 37 °C in a humidified atmosphere with 5% CO_2 for the respective time intervals. All cell experiments were performed 3 times using different cell passages.

2.3.2. *Cell viability*

Mitochondrial dehydrogenase activity was measured by MTT assay (3-(4,5-dimethylthiazol-2-yl)-2,5-diphenyltetrazolium bromide) to investigate cell viability of cells growing on specimens. After incubation of MG-63 cells for 24 h on the different surfaces to evaluate the initial cell reaction to the bioglass, specimens were transferred to a new well-plate and MTS solution (CellTiter 96 ONE-Solution Cell Proliferation Assay, Promega, Madison, USA) with culture medium was added (1:5) to each specimen. A blank group containing a specimen with culture medium without cells and a control group with cells growing on well bottom were additionally tested. After 80 min, supernatants were transferred to a 96-well plate (for each specimen 3 × 80 μl were analyzed). The optical density (OD) was recorded at 490 nm with a micro-plate reader (Anthos, Mikrosysteme, Krefeld, Germany). Relative cell viability was calculated using the following equation:

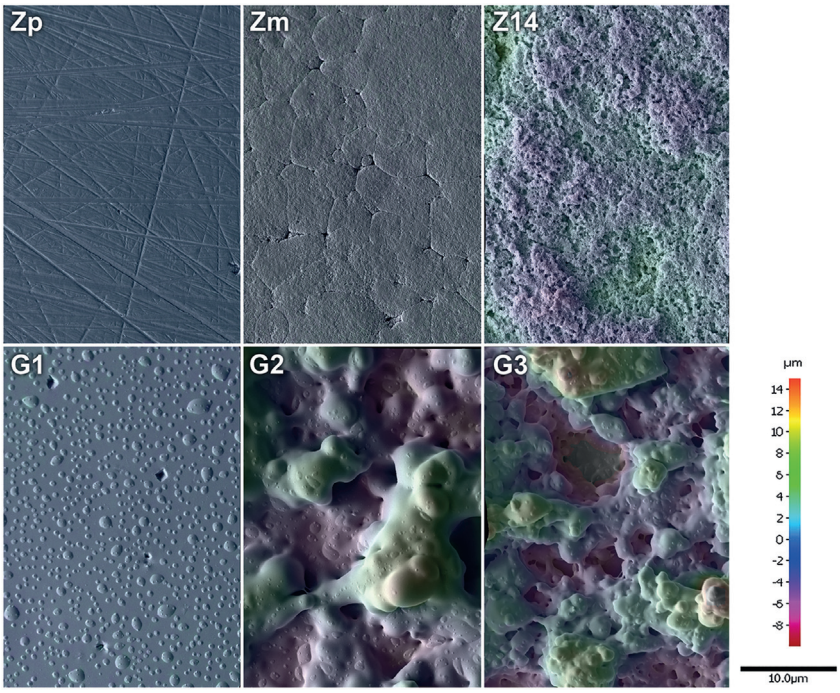

Fig. 1 – 3D surface morphologies of zirconia specimens Zp, Zm, Z14, and bioglass-coated specimens G1, G2, G3 (SEM 1000×).

$$\text{Relativecellviability} = (OD_{specimen} - OD_{blankspecimen})/(OD_{control} - OD_{blankcontrol}).$$

2.3.3. *Cell spreading*

Cell spreading was assessed on all surfaces after 30 min and 24 h, respectively. Due to the opaque material properties of the zirconia specimens, osteoblasts were labelled using red fluorescent dye (PKH-26, Sigma-Aldrich, Steinheim, Germany) prior to seeding. After 30 min or 24 h, cells were rinsed twice with PBS (dulbecco's phosphate buffered saline, Sigma-Aldrich, Steinheim, Germany) fixed with 4% paraformaldehyde for 10 min at RT, rinsed again with PBS and embedded with mounting medium (Fluoroshield with DAPI, Sigma-Aldrich) and a cover slip. Cells were examined with a water immersion objective (C Apochromat 40×, Carl Zeiss, 1.20 W Korr M27) at a wavelength of 546 nm by a confocal laser scanning microscope (LSM780, Carl Zeiss, Oberkochen, Germany). Mean spreading area in μm^2 of 40 cells per specimen was then analyzed using image processing software (ImageJ, v2.0.0).

2.3.4. *Cell morphology*

Cell morphology after 30 min and 24 h was visualized using SEM (FEI Nova NanoSEM230, Thermo Fisher Scientific). Cells on the specimens were rinsed with PBS after the respective time intervals, fixed with 2.5% glutaraldehyde (Merck KGaA) for 15 min at RT, rinsed with PBS, dehydrated with ethanol (30%, 50%, 70%, 90%, abs.), dried in a desiccator with silica gel and gold-sputtered. Critical point drying was not performed to prevent bioglass surfaces from further corrosion.

2.4. *Statistical analysis*

Data of surface roughness, contact angle, cell viability and cell spreading were analyzed separately for normal distribution. With data of roughness parameter Rz a logarithmic transformation was performed due to variations in standard deviations. One-way ANOVA was then applied followed by post-hoc Fisher LSD to test for differences between the substrates ($p < 0.05$) (StatPlus Pro, v6.1.25).

Table 2 – 2D/3D roughness parameters arithmetical mean height (Ra, Sa) and maximum height of profile (Rz, Sz) and water contact angle (WCA) on the specimens.

	Zp	Zm	Z14	G1	G2	G3
Ra (µm)	0.1 ± 0.0^{A}	0.2 ± 0.0^{A}	1.4 ± 0.3^{B}	1.3 ± 0.2^{B}	5.9 ± 0.7^{C}	5.9 ± 0.6^{C}
Rz (µm)	0.6 ± 0.3^{A}	1.6 ± 0.2^{B}	8.8 ± 0.3^{C}	5.9 ± 0.5^{C}	32.3 ± 5.0^{D}	29.9 ± 8.8^{D}
Sa (µm)	0.07	0.23	1.20	0.83	3.90	3.70
Sz (µm)	1.20	2.50	13.20	4.20	23.70	29.30
WCA (°)	67.8 ± 6.0^{A}	68.6 ± 5.4^{A}	44.8 ± 7.4^{B}	32.1 ± 4.9^{C}	40.1 ± 5.3^{D}	36.9 ± 5.5^{E}

Statistically differing groups ($p < 0.05$) are indicated with superscript letters within the same parameter (horizontal comparison).

3. Results

3.1. Surface characterization

The surface morphologies of zirconia Zp, Zm and Z14 as well as glass-coated G1–G3 specimens are displayed in Fig. 1. On Zp polishing grooves are visible while zirconia crystals are not exposed. Zm displays the typical structure of sintered zirconia revealing partially connected grain boundaries as well as a nanostructuring due to the exposed zirconia crystals. Z14 reveals a micro-structured surface with exposed zirconia crystals. All bioglass surfaces display bubbly topographies owed to the spray coating process. While G1 displays a rather plane surface, the topography is enhanced for G2 and G3.

2D and 3D roughness values of the specimens are given in Table 2. Zp and Zm displayed similar Ra/Sa values between 0.07–0.23 μm, so did Z14 and G1 (0.83–1.40 μm) and G2 and G3 (3.7–5.9 μm). Ra and Rz of the respective specimens correlated linearly ($y = 0.1887x$, $R^2 = 0.994$), also Sa and Sz ($y = 7.104x$, $R^2 = 0.927$) and Ra and Sa ($y = 0.650$, $R^2 = 0.992$).

Contact angle of water on the specimens was generally lower on bioglass coated specimens than on zirconia (Table 2). Significantly higher contact angle values were measured on Zp = Zm > Z14 > G2 > G3 > G1 ($p < 0.05$).

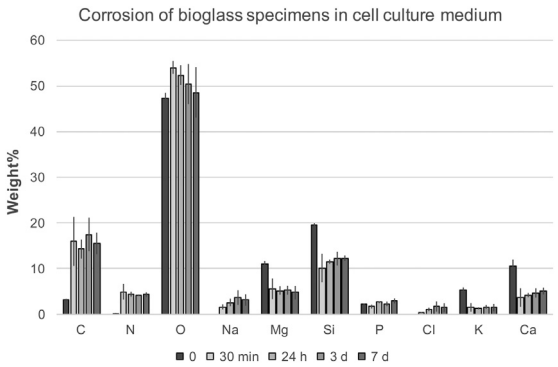

Fig. 2 – EDX surface analysis of pooled bioglass-coated surfaces G1–G3 at 20 kV after storage in complete cell culture medium DMEM + 10%FCS for 30 min, 24 h, 3 d, and 7 d revealing elements present at the bioglass surface (n = 6).

EDX analysis revealed a change in elements present on the glass surfaces after storage in cell culture medium up to 7 d (Fig. 2). The storage in cell culture medium resulted in a statistically significant increase of C and N on the glass surfaces when compared to the surfaces that were not subjected to the suspension ($p < 0.05$). Na and Cl also tended to increase after 30 min but the increase was not statistically different until

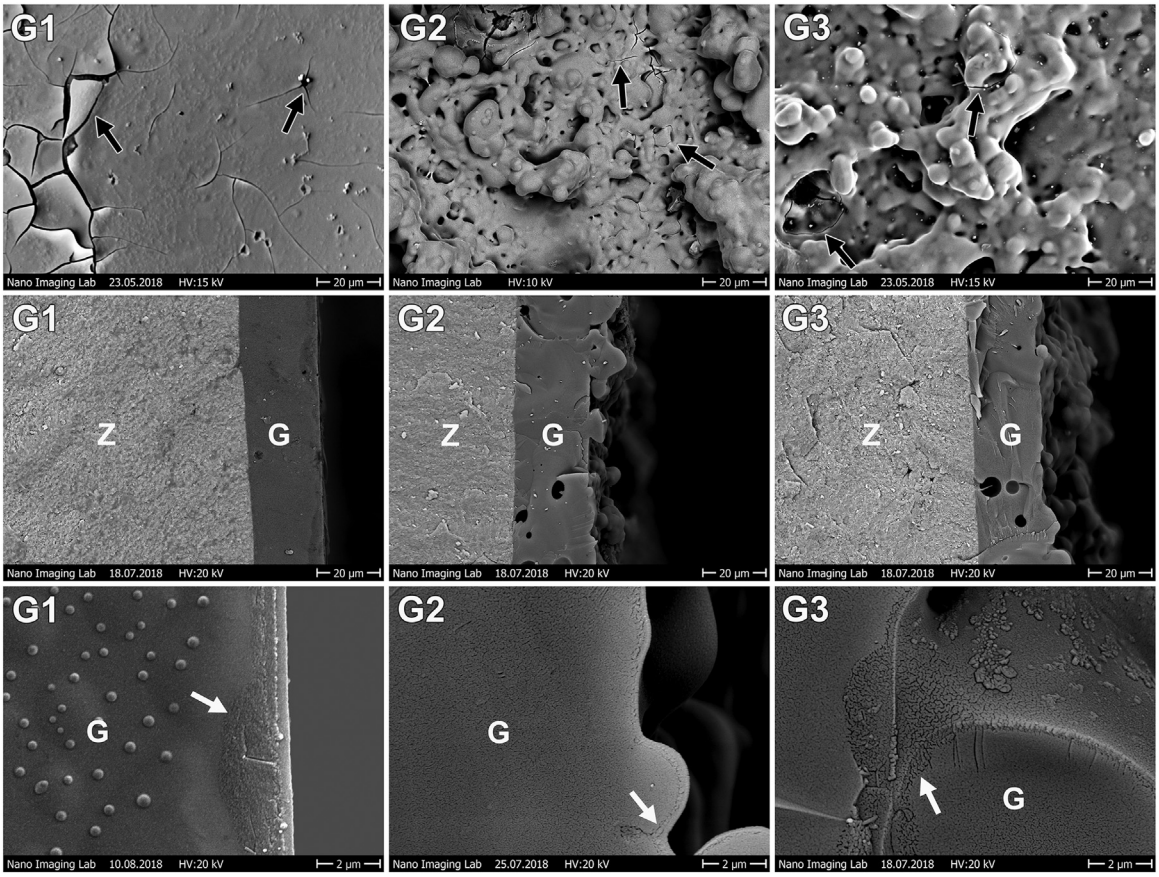

Fig. 3 – Surface corrosion after 7 d storage in cell culture medium of bioglass-coated specimens G1–G3. Upper row: bioglass surfaces, black arrows indicate cracks (1000×); second row: z-cut of specimens, left zirconia (Z), right bioglass layer (G) (1000×); lower row: close-up z-cut of corrosion layer indicated with white arrows at the bioglass surface of the specimens (10,000x).

storage for 24 h ($p > 0.05$). Oxygen was statistically significantly increased after 30 min and then decreased again. The presence of Mg, Si, K, and Ca was significantly decreased ($p < 0.05$). The obtained surfaces after storage for 7 d in cell culture medium are given in Fig. 3. Crack formation was detectable on the SEM images of the substrates. When specimens were broken in half and EDX analysis was performed through the cross-sectional area of the glass coating (z-cut), changes in composition as displayed in Fig. 2 were only observed within the superficial 1–2 μm (Fig. 3).

3.2. *Cell behavior*

The relative cell viability after 24 h was significantly higher for Zp than for all other specimens ($p < 0.001$) (Fig. 4). The mean cell spreading area after 30 min and 24 h on the different specimens is displayed in Fig. 5. For the interpretation of the results it has to be considered that obtaining focused images with LSM of cells on specimens with a high surface roughness (G2, G3) was difficult. Due to the adaption of the cells to the microstructures of certain specimens (Z14, G2, G3), the actual basal spreading area might be slightly higher than measured. Corresponding SEM images of cell morphologies after 30 min and 24 h are presented in Fig. 6. Initial cell spreading after 30 min was accelerated on flat zirconia surfaces Zp and Zm. On Z14 cells started to spread into the porous structures where they anchor their filopodia. Cells on glass-surfaces are still in spherical shape, just starting their spreading. After 24 h, cells spread flat on Zp, Zm and G1. Cells on Z14 nestled into the porous structures of zirconia while cells on G2 and G3 spanned over the gaps of the micro-structured glass surfaces.

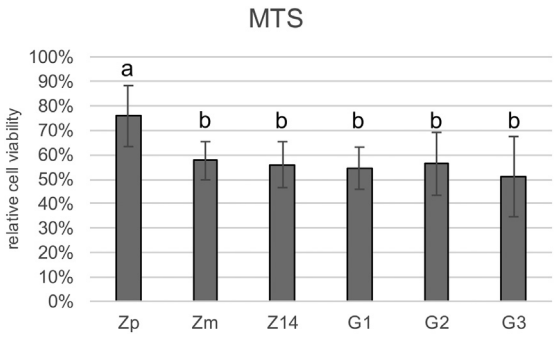

Fig. 4 – Relative cell viability determined with MTS assay after 24 h. Three independent experiments were performed with three measurements per specimen (n = 9). The relative cell viability refers to the control cells grown on well bottom. Statistically significant differences determined with post.hoc test Fisher LSD are indicated with differing letters ($p < 0.05$).

4. Discussion

The objective of the present study was to evaluate osteoblast behavior on bioactive glass PC-XG3 and to further characterize its corrosion. The first hypothesis that cell viability of human osteoblasts will be increased on PC-XG3 coated surfaces compared to zirconia was rejected because cell viability was similar on glass surfaces as on Zm and Z14 and even significantly lower than on Zp. The second hypothesis that cell spreading will be accelerated on PC-XG3 surfaces compared to zirconia surfaces was also rejected. Analysis of cell spreading area and morphology revealed that cell spreading after 30 min was further enhanced on zirconia than on glass surfaces.

The specimens tested in the present study presented roughness parameters classified as smooth (Zp, Zm) to moderately rough (Z14, G1) to rough surfaces (G2, G3) as previously defined [20]. Currently available zirconia implants display minimally to moderately rough surfaces with Sa values ranging from 0.73 to 1.27 μm [21]. A certain roughness seems to be required for the mechanical anchorage of the implant in the bone, however, the ideal surface topography of zirconia implants has not yet been identified [22].

Initial water contact angles >90° of implant surfaces are considered unfavorable for the initial biological response in blood contact [23,24]. All surfaces in the present study displayed hydrophilic properties that are defined as contact

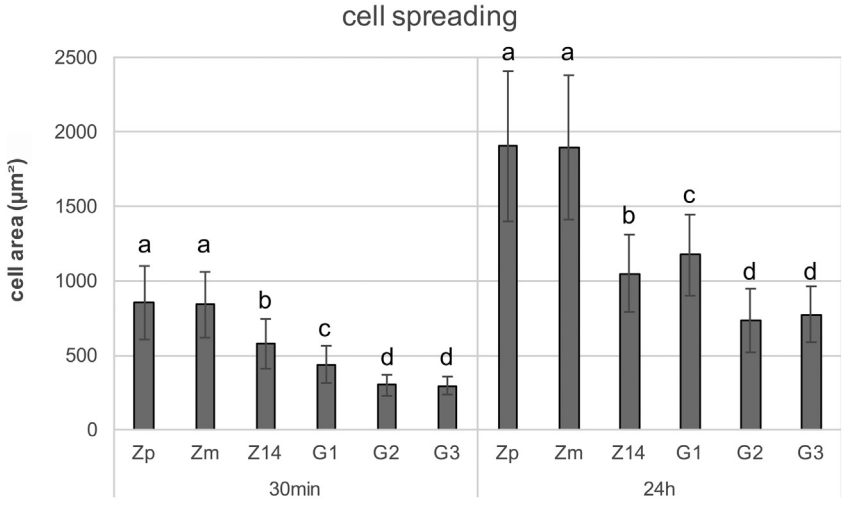

Fig. 5 – Cell spreading after 30 min and 24 h on all specimens (n = 120). Statistically significant differences between specimens within 30 min or 24 h obtained with post.hoc test Fisher LSD are indicated with differing letters ($p < 0.05$).

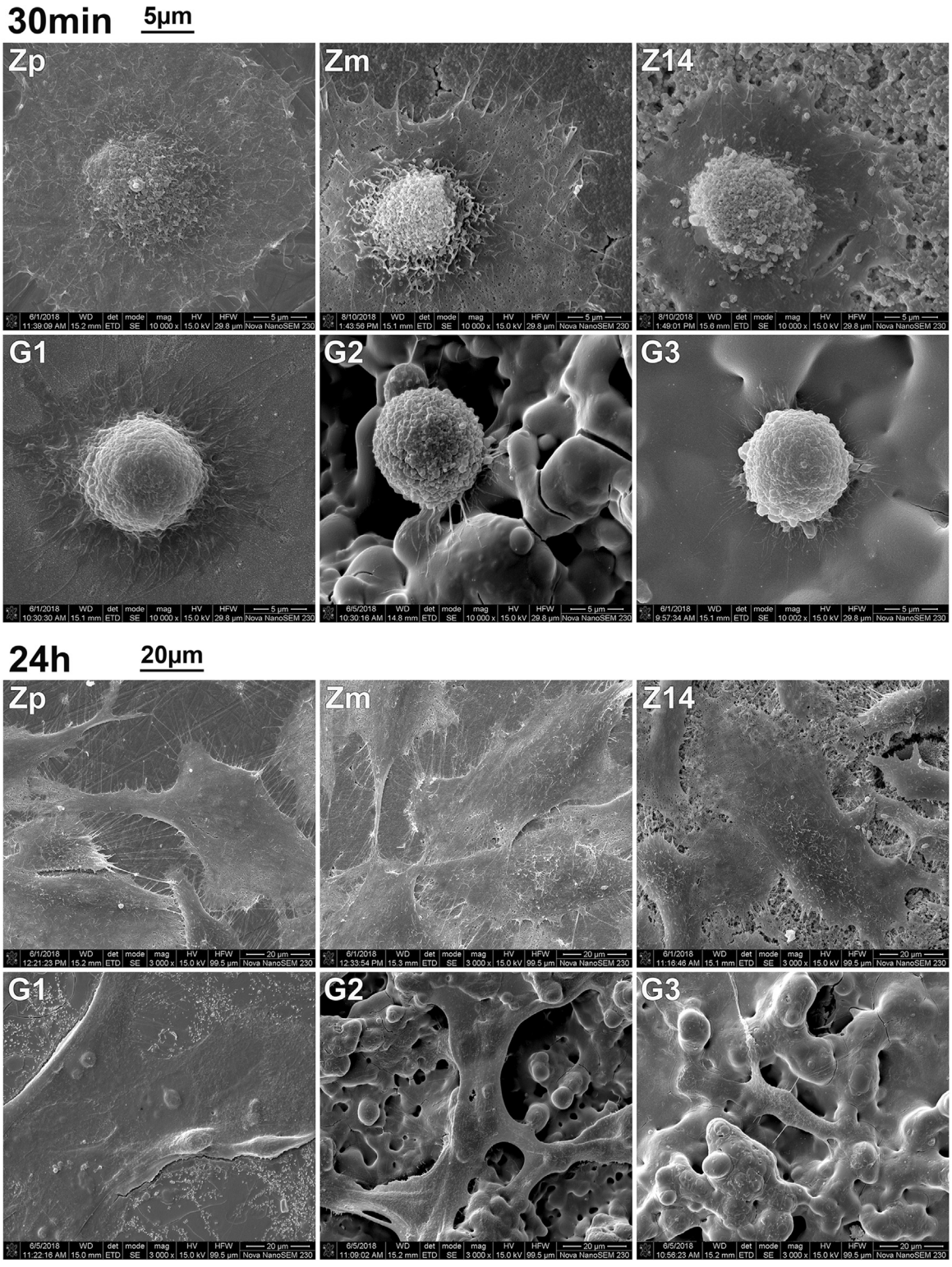

Fig. 6 – Cell morphology of MG-63 osteoblasts after 30 min (10,000×, bar 5 µm) and 24 h (3000×, bar 20 µm) on zirconia surfaces Zp, Zm, Z14 and bioglass-coated surfaces G1–G3 obtained with SEM.

angles between 10° and 90° [23]. Although glass-coated surfaces revealed significantly lower contact angles than zirconia, it has to be considered that the contact angle is influenced by the surface's chemistry as well as surfaces' microstructure and roughness [23,25]. Silica containing glasses generally display lower contact angles with water than zirconia due to their increased polar surface energy component [26].

In a previous study where the bioglasses PC-XG3 and 45S5 were stored in SBF solution, a Si-rich layer of 20 µm covered by a CaP-rich layer of about 10 µm was formed on the sur-

faces after 14 d [19]. Additionally, carbonated hydroxyapatite was found after 3.5 d–7 d [19]. In the present study, the effect of the storage in cell culture medium on the corrosion of the glass surfaces was evaluated. Cell culture medium contains DMEM, which is mainly a mixture of inorganic salts and amino acids, as well as fetal calf serum. The reaction of the glass-surface to the cell culture medium was different than to SBF. Already after 30 min an accumulation of C, N, Na, and Cl was observed with EDX analysis on the glass surfaces. A decrease in concentration of Mg, Si, K, and Ca was detected as a result of the corrosive reaction. Hence, the corrosion process was already initiated after 30 min storage and prolonged storage up to 7 d did not seem to basically change the surface composition. This altered reaction compared to previous findings might be due to the content of serum in the cell culture medium that resulted in an accumulation of proteins on the specimens' surfaces as it has been previously described for bioglass 45S5 [27]. Additionally, cell culture medium does not contain the same amount of electrolytes as SBF (especially Ca and P ions) that precipitate on the surface of the glass and provide potential ionic reaction partners. Consequently, an accumulation of Ca and P as an indicator for hydroxyapatite or hydroxyl carbonated apatite formation [13] on the PCX-G3 surface did not occur.

The formation of cracks and delamination of the glass surfaces are a typical corrosion process of bioglass as shown in the literature [17,19,27,28].

Cell behavior on the specimens was assessed using the human osteoblast-like cell line MG-63 that is reported to display similar cellular reactions regarding morphological behavior, adhesion and signaling properties on biomaterials as primary human osteoblasts [29,30]. Cell viability of the cells revealed to be accelerated on Zp compared to cells on all other surfaces that displayed similar metabolic activities. Further investigations are required to explain this phenomenon. Cells on Zp might have been stimulated by the submicrometer grooves (Fig. 1) that are not present on Zm. On silicon wafers it has been previously demonstrated that submicrometer grooves, especially a 600 nm pitch induce faster initial cell adhesion of MC3T3-E1 osteoblasts [31].

Initial cell spreading after 30 min was clearly promoted on zirconia compared to glass-coated specimens. This might be due to the degenerative process of bioglass making it difficult for cells to adhere on the instable substrate. Additionally, an increased roughness of the specimens resulted in a lower initial cell spreading area. It has been speculated that ridges and valleys on rough surface may exert stronger constraints on cells than smooth surfaces which therefore only require weak restraints; thus the cells on the smooth surface try to spread widely to stabilize themselves on the substrate [32]. After 24 h, cell spreading on smooth surfaces Zp and Zm was significantly higher compared to Z14, confirming previous findings for primary human osteoblast on machined and cer.face 14 zirconia surfaces [33]. Cell spreading on Z14 was significantly lower than for G1, which was due to the cells' adaption on Z14 into the surface structures, hence the image of the center and not the basal cell diameter was taken by LSM. On G2 and G3 cells span through the ridges and displayed a cuboidal shape with long cellular extensions (Fig. 6). Similar cell behavior has been previously observed for cells on sandblasted titanium surfaces that also exhibited rough surface morphologies (Ra = 6.07 μm) [34].

Further studies are required to assess the contribution of submicrometer and micrometer surface structure levels on zirconia to create an implant surface with ideal biological and osseointegration capabilities.

5. Conclusion

Analysis of cell viability, cell spreading area, and morphology revealed that initial cell behavior of human osteoblasts is not accelerated by the bioglass-coated surface PC-XG3 when compared to zirconia. Since initial spreading quality to a biomaterial is a crucial factor that will determine the subsequent cell function, proliferation, differentiation, and viability it can be concluded that a coating of zirconia implants with this bioactive glass will unlikely enhance the osseointegration behavior in vivo.

Funding

This work was in part supported by the ITI foundation Switzerland (research grant 1280_2018).

Acknowledgements

The authors are grateful to the team at the Department of Cell Biology, Rostock for the laboratory assistance.

REFERENCES

[1] Osman R, Swain M. A critical review of dental implant materials with an emphasis on titanium versus zirconia. Materials 2015;8:932–58.
[2] Pieralli S, Kohal RJ, Jung RE, Vach K, Spies BC. Clinical outcomes of zirconia dental implants: a systematic review. J Dent Res 2017;96:38–46.
[3] Hashim D, Cionca N, Courvoisier DS, Mombelli A. A systematic review of the clinical survival of zirconia implants. Clin Oral Investig 2016;20:1403–17.
[4] Balmer M, Spies BC, Vach K, Kohal RJ, Hämmerle CHF, Jung RE. Three-year analysis of zirconia implants used for single-tooth replacement and three-unit fixed dental prostheses: a prospective multicenter study. Clin Oral Implants Res 2018;29:290–9.
[5] Kniha K, Schlegel KA, Kniha H, Modabber A, Hölzle F, Kniha K. Evaluation of peri-implant bone levels and soft tissue dimensions around zirconia implants—a three-year follow-up study. Int J Oral Maxillofac Surg 2018;47:492–8.
[6] Piconi C, Maccauro G. Zirconia as a ceramic biomaterial. Biomaterials 1999;20:1–25.
[7] Wennerberg A, Albrektsson T. Effects of titanium surface topography on bone integration: a systematic review. Clinical Oral Implants Research 2009;20:172–84.
[8] Fischer J, Schott A, Märtin S. Surface micro-structuring of zirconia dental implants. Clin Oral Implants Res 2016;27:162–6.
[9] Lambert F, Mainjot A. One-Tooth One-Time (1T1T): a straightforward approach to replace missing teeth in the posterior region. J Oral Implantol 2017;43:371–7.

[10] Krajewski A, Malavolti R, Piancastelli A. Albumin adhesion on some biological and non-biological glasses and connection with their Z-potentials. Biomaterials 1996;17:53–60.
[11] Gomez-Vega JM, Saiz E, Tomsia AP. Glass-based coatings for titanium implant alloys. J Biomed Mater Res 1999;46:549–59.
[12] Hench LL. The story of Bioglass. J Mater Sci Mater Med 2006;17:967–78.
[13] Fernandes HR, Gaddam A, Rebelo A, Brazete D, Stan GE, Ferreira JMF. Bioactive glasses and glass-ceramics for healthcare applications in bone regeneration and tissue engineering. Materials 2018;11.
[14] Jones JR. Review of bioactive glass: from Hench to hybrids. Acta Biomater 2013;9:4457–86.
[15] Wilson J, Pigott GH, Schoen FJ, Hench LL. Toxicology and biocompatibility of bioglasses. J Biomed Mater Res 1981;15:805–17.
[16] Granito RN, Rennó AC, Ravagnani C, Bossini PS, Mochiuti D, Jorgetti V, et al. In vivo biological performance of a novel highly bioactive glass-ceramic (Biosilicate®): a biomechanical and histomorphometric study in rat tibial defects. J Biomed Mater Res B Appl Biomater 2011;97:139–47.
[17] Ferraris M, Verné E, Appendino P, Moisescu C, Krajewski A, Ravaglioli A, et al. Coatings on zirconia for medical applications. Biomaterials 2000;21:765–73.
[18] Fischer J, Stawarczyk B, Tomic M, Strub JR, Hämmerle CH. Effect of thermal misfit between different veneering ceramics and zirconia frameworks on in vitro fracture load of single crowns. Dent Mater J 2007;26:766–72.
[19] Kirsten A, Hausmann A, Weber M, Fischer J, Fischer H. Bioactive and thermally compatible glass coating on zirconia dental implants. J Dent Res 2015;94:297–303.
[20] Wennerberg A, Ide-Ektessabi A, Hatkamata S, Sawase T, Johansson C, Albrektsson T, et al. Titanium release from implants prepared with different surface roughness. Clin Oral Implants Res 2004;15:505–12.
[21] Beger B, Goetz H, Morlock M, Schiegnitz E, Al-Nawas B. In vitro surface characteristics and impurity analysis of five different commercially available dental zirconia implants. Int J Implant Dent 2018;4:13.
[22] Pieralli S, Kohal RJ, Lopez Hernandez E, Doerken S, Spies BC. Osseointegration of zirconia dental implants in animal investigations: a systematic review and meta-analysis. Dent Mater 2018;34:171–82.
[23] Rupp F, Liang L, Geis-Gerstorfer J, Scheideler L, Hüttig F. Surface characteristics of dental implants: a review. Dent Mater 2018;34:40–57.
[24] Schwarz F, Wieland M, Schwartz Z, Zhao G, Rupp F, Geis-Gerstorfer J, et al. Potential of chemically modified hydrophilic surface characteristics to support tissue integration of titanium dental implants. J Biomed Mater Res B Appl Biomater 2009;88:544–57.
[25] Giljean S, Bigerelle M, Anselme K, Haidara H. New insights on contact angle/roughness dependence on high surface energy materials. Appl Surf Sci 2011;257:9631–8.
[26] Agathopoulos S, Nikolopoulos P. Wettability and interfacial interactions in bioceramic-body-liquid systems. J Biomed Mater Res 1995;29:421–9.
[27] Ducheyne P, Qiu Q. Bioactive ceramics: the effect of surface reactivity on bone formation and bone cell function. Biomaterials 1999;20:2287–303.
[28] Plewinski M, Schickle K, Lindner M, Kirsten A, Weber M, Fischer H. The effect of crystallization of bioactive bioglass 45S5 on apatite formation and degradation. Dent Mater 2013;29:1256–64.
[29] Czekanska EM, Stoddart MJ, Ralphs JR, Richards RG, Hayes JS. A phenotypic comparison of osteoblast cell lines versus human primary osteoblasts for biomaterials testing. J Biomed Mater Res A 2014;102:2636–43.
[30] Staehlke S, Rebl H, Finke B, Mueller P, Gruening M, Nebe JB. Enhanced calcium ion mobilization in osteoblasts on amino group containing plasma polymer nanolayer. Cell Biosci 2018;8:22.
[31] Lamers E, te Riet J, Domanski M, Luttge R, Figdor CG, Gardeniers JG, et al. Dynamic cell adhesion and migration on nanoscale grooved substrates. Eur Cell Mater 2012;23:182–93.
[32] Anselme K, Bigerelle M, Noël B, Iost A, Hardouin P. Effect of grooved titanium substratum on human osteoblastic cell growth. J Biomed Mater Res 2002;60:529–40.
[33] Bergemann C, Duske K, Nebe JB, Schöne A, Bulnheim U, Seitz H, et al. Micro-structured zirconia surfaces modulate osteogenic marker genes in human primary osteoblasts. J Mater Sci Mater Med 2015;26:26.
[34] Lüthen F, Lange R, Becker P, Rychly J, Beck U, Nebe JB. The influence of surface roughness of titanium on beta1- and beta3-integrin adhesion and the organization of fibronectin in human osteoblastic cells. Biomaterials 2005;26:2423–40.